Green Fabrication of Porous Chitosan/Graphene Oxide Composite Xerogels for Drug Delivery

Yunping Chen,[1,2] Yuanyuan Qi,[1,3] Xingbin Yan,[1,3] Haibing Ma,[1,4] Jiangtao Chen,[1,3]
Bin Liu,[2] Qunji Xue[3]

[1]Laboratory of Clean Energy Chemistry and Materials, Lanzhou Institute of Chemical Physics, Chinese Academy of Sciences, Lanzhou 730000, People's Republic of China
[2]School of Stomatology, Lanzhou University, Lanzhou 730000, People's Republic of China
[3]State Key Laboratory of Solid Lubrication, Lanzhou Institute of Chemical Physics, Chinese Academy of Sciences, Lanzhou 730000, People's Republic of China
[4]Gansu Province Hospital of Traditional Chinese Medicine, Lanzhou 730000, People's Republic of China
Correspondence to: X. Yan (E-mail: xbyan@licp.cas.cn) or B. Liu (E-mail: liubkq@lzu.edu.cn)

ABSTRACT: Porous chitosan (CS)/graphene oxide (GO) composite xerogels were prepared through a simple and "green" freeze-drying method. Scanning electron microscopy, Fourier transform infrared spectrometry, powder X-ray diffraction, and compressive strength measurements were performed to characterize the microstructures and mechanical properties of as-prepared composite xerogels. The results show that the incorporation of GO resulted in an observable change in the porous structure and an obvious increase in the compressive strength. The abilities of the composite xerogels to absorb and slowly release an anticancer drug, doxorubicin hydrochloride (DOX), in particular, the influence of different GO contents, were investigated systematically. The porous CS/GO composite xerogels exhibited efficient DOX-delivery ability, and both the adsorption and slow-release abilities increased obviously with increasing GO content. Additionally, the best adsorption concentration of DOX was 0.2 mg/mL, and the cumulative release percentage of DOX from the xerogels at pH4 much higher than that at pH 7.4. Therefore, such porous CS/GO composite xerogels could be promising materials as postoperation implanting stents for the design of new anticancer drug-release carriers. © 2013 Wiley Periodicals, Inc. J. Appl. Polym. Sci. **2014**, *131*, 40006.

INTRODUCTION

Cancer is becoming more and more common, but in many cases, malignant tumors are detected only at advanced stages, and then, the majority of patients needed surgery and postoperative chemotherapy drug treatment. However, chemotherapeutic drugs become increasingly toxic to healthy cells. To improve this condition, polymer scaffolds in the surgical area as drug carriers, have attracted more and more attention, especially in hard tissue, such as bone tumors. In such a case, a polymer scaffold can be used as a drug-delivery system to provide the sustained release of small doses of the drug to maintain the desired therapeutic range, localize the delivery of the drug to a particular part of the body, reduce the need for follow-up care, prevent drugs from being rapidly destroyed by the body, and increase patient comfort.[1–3]

As a natural biopolymer, chitosan (CS) is a high-molecular-weight linear cationic polysaccharide composed mainly of 2-amino-2-deoxy(1,4)-β-D-glucopyranose residues (or D-glucosamine units) and derived from the extensive deacetylation of chitin. CS is plastic and organic. Because of its good biocompatibility, biodegradability, low immunogenicity, and antibacterial properties,[4–6] CS has been applied in tissue engineering scaffolds,[7] biomedical products,[8] and matrixes for the controlled release of drugs and genes. In particular, a growing field of interest in polymer matrixes has been found in applications for local drug release at the implanted site. As a low-cost and nontoxic natural biomaterial, CS has also been considered to be a "green" adsorbent because it contains various functional groups, such as amino and hydroxyl groups.[9]

Recently, graphene and its derivatives have attracted great research interest because of their unique physicochemical

Additional Supporting Information may be found in the online version of this article.

properties. They have shown various potential applications in electronics, energy, composites, and biomedical areas.[10–12] Graphene oxide (GO) is one of the most important graphene derivatives,[13] and it has a high Young's modulus and hardness, excellent flexibility, good biocompatibility, and low cost compared to carbon nanotubes; this makes it an effective reinforced component of new composite materials.[14] GO sheets can attach many oxygen-containing hydrophilic functional groups, including carboxyl (—COOH) and hydroxyl (—OH) groups,[15–17] and the surfaces of GO sheets are highly negatively charged when they are dispersed in water; this results in the ionization of carboxylic acid and phenolic hydroxyl groups on the surfaces of GO sheets.[18] The hydrophilicity of GO sheets and electrostatic repulsion among GO sheets lead to the individual sheet level dispersion of GO in water.

In bio-application fields, the *in vivo* and *in vitro* cytotoxicity of GO-based composites is an important fundamental issue. Several research groups have studied the toxicity of GO-based materials. Chang et al.[19] reported that no obvious cytotoxicity of GO in A549 adenocarcinomic human epithelial cells at low GO concentrations, whereas high concentrations of GO could reduce the viabilities of cells. Zhang et al.[20] found that pristine GO exhibited a dose-dependent toxicity to various types of cells. In contrast, surface modifications of GO with hydrophilic macromolecules, such as CS,[21] poly(ethylene glycol),[22] and even proteins,[23] were reported to remarkably decrease its cytotoxic effects. Liao et al.[21] reported that GOs with small sizes showed strong hemolytic activity, which could be nearly eliminated when GO was coated with CS. Magrez et al.[24] also demonstrated similar results, in which GO coated with dextran remarkably improved the *in vitro* biocompatibility and notably reduced cell growth inhibition effects. These results were mainly due to the biocompatible polymer coating on GO, which offered GO excellent solubility and stability in physiological solutions, attenuating its direct interactions with cell membranes, reducing nonspecific binding with biomolecules, and resulting in much lower *in vitro* cytotoxicity to cells.[25]

Up to now, some reports have shown that CS/GO composites combine the advantages of both CS and GO materials and possess new properties. Bao et al.[26] successfully functionalized GO sheets with CS via a facile amidation process. The CS-grafted GO (GO–CS) sheets had a good aqueous solubility and as a novel nanocarrier, the GO–CS sheets possessed a superior loading capacity for camptothecin (CPT) drug and DNA. Rana et al.[27] also synthesized CS-functionalized GO sheets and successfully loaded Ibuprofen (IBU) and 5-fluorouracil or 5-flouro-2, 4(1h, 3h)pyrimidinedione (5-FU) on GO–CS sheets, which exhibited controlled release behavior and long-term biocompatibility. These studies showed that the CS functionalization could increase the biocompatibility and the drug-delivery ability of bare GO sheets. Moreover, Pan et al.[28] studied GO as a new filler to reinforce the CS matrix. With the incorporation of 1 wt % GO, both the fracture strength and the tensile modulus of the nanocomposites were remarkably enhanced by 93 and 51%, respectively. Similarly, Depan et al.[29] successfully incorporated GO into a network of CS scaffolds; they displayed a combination of high modulus and high strength. Meanwhile, the authors

observed that the degradation products from pure CS and CS–GO scaffolds were cytocompatible and did not impart a significant level of toxicity. In addition, CS is one of the most promising adsorbents, and there have been studies on strengthening the adsorption performance for heavy metals of CS through the addition of GO. Zhang and coworkers[30,31] prepared ordered, porous CS–gelatin/GO monoliths with over 97% porosity, which exhibited extremely high adsorption abilities for metal ions.

Doxorubicin hydrochloride (DOX) is a cytotoxic and anthracycline antibiotic used in antimitotic chemotherapy. It is commonly used to treat bone cancer.[1] Because of the narrow therapeutic index of DOX, it is impossible that a substantial increase in the systematic dose of the drug will cause a high concentration at the bone cancer place. It also causes side effects and the occurrence of drug resistance. Currently, DOX is incorporated into physically self-assembled structures (e.g., liposomes, micelles) and polymer–drug conjugates.[32–35] Although the therapeutic effects are enhanced, serious problems, such as low encapsulation efficiency, drug leakage, and the low stability of DOX-loaded liposomes or micelles, have been generated.

In this study, we prepared a series of porous CS/GO composite xerogels by means of a simple and fully green freeze-drying technique. This is the first time CS/GO xerogels have been investigated as a potential implantable delivery material. The microstructure and physicochemical properties of the resulting xerogels were investigated by scanning electron microscopy (SEM), Fourier transform infrared (FTIR) spectrometry, X-ray diffraction (XRD), and mechanical testing. The effect of the DOX concentration and GO content on the adsorption of DOX of the CS/GO xerogels were investigated. The release behavior of DOX was explored as a function of the GO content and the pH of phosphate-buffered saline (PBS). It has been reported that CS functionalization can increase the drug-delivery ability of GO sheets.[26,27] Conversely, our results show that a small quantity of GO also enhanced this ability of CS.

EXPERIMENTAL

Materials

CS (5.63×10^3 kDa) with a 91% degree of deacetylation was supplied by Qingdao Hecreat Bio-Tech Co., Ltd. (China). Graphite powder (325 mesh) was purchased from Qingdao Huatai Tech. Co., Ltd. (China). DOX was purchased from Shenzhen Main Luck Pharmaceuticals, Inc. (China). All of the chemicals were used without further purification. Throughout the experiments, double-distilled water was used.

Synthesis of GO

GO was prepared according to the method described by Hummer with a modification.[36] In a typical synthesis, graphite powder (3 g, 325 mesh) was put into an 80°C solution of concentrated H_2SO_4 (12 mL), $K_2S_2O_8$ (2.5 g), and P_2O_5 (2.5 g). The mixture was kept at 80°C for 4.5 h with a hotplate. Successively, the mixture was cooled to room temperature, diluted with 0.5 L of H_2O, and left overnight. Then, the mixture was filtered and washed with H_2O with a 0.45-μm Millipore filter to remove the residual acid. The product was dried under ambient conditions. This pre-oxidized graphite was then subjected to

oxidation by Hummers' method, described as follows. Pretreated graphite powder was put into cold (0°C) concentrated H_2SO_4 (120 mL). Then, $KMnO_4$ (15 g) was added gradually under stirring, and the temperature of the mixture was kept to below 20°C by cooling. Successively, the mixture was stirred at 35°C for 2 h and then carefully diluted with 250 mL of H_2O. After that, the mixture was stirred for 2 h, and then, an additional 0.7 L of H_2O was added. Shortly, 20 mL of 30% H_2O_2 was added to the mixture. The resulting brilliant yellow mixture was filtered and washed with a 10 wt % HCl aqueous solution (1 L) to remove metal ions; this was followed by repeated washing with H_2O to remove the acid until the pH of the filtrate was neutral. Then, the GO slurry was dried in a vacuum oven at 60°C after the dialysis.

Preparation of CS and CS/GO Xerogels

Different amounts of GO (4, 12, and 20 mg) were added to 2% (v/v) acetic acid solutions, and then, 0.4 g of CS was added to each and allowed to dissolve; this was followed by ultrasonic treatment for about 10 min in an ice bath. The mixtures (20 mL) were then poured into glass culture dishes (10 cm in diameter) and evenly distributed in the dishes. Then, they were frozen under −50°C for 2 h, and the resulting solid-state mixtures were then transferred to freeze-drying vessels and freeze-dried for 48 h *in vacuo* (<20 Pa) to obtain a series of porous CS/GO xerogels with GO contents of 1, 3, and 5 wt %. Similarly, the porous CS xerogel without GO was prepared by the same procedure. After that, the dried CS and CS/GO xerogels were immersed in a dilute NaOH ethanol solution. After mild oscillation, they were taken out and repeatedly rinsed with anhydrous ethanol until the pH of the solution was close to neutral. The treated porous CS and CS/GO xerogels were dried again in the freeze drier for 4 h and then collected and stored in a desiccator for further analysis.

Morphological and Structural Characterization

A Nanoscope III multimode atomic force microscope (Veeco) was used to characterize the thickness of as-prepared GO sheets. Transmission electron microscopy (JEOL, JEM-2010) was used to investigate the morphology of as-prepared GO sheets with an accelerating voltage of 200 kV. A PerkinElmer PHI-5702 multifunctional X-ray photoelectron spectroscope (Physical Electronics, United States) was used to analyze the surface components of the GO with Al Kα radiation (photon energy = 1476.6 eV) as the excitation source and the binding energy of Au (84.00 eV) as the reference. SEM (JSM-5600LV) was conducted to investigate the morphologies of the as-made xerogels. The crystallinity and microstructure of the xerogels were characterized by XRD (Philips X' Pert Pro) and FTIR spectrometry (Bruker IFS66V).

Thermogravimetric Analysis (TGA)

The porous CS/GO composite xerogels were dried in a freeze drier, and then, TGA was performed on a STA 449C instrument under a nitrogen atmosphere at a heating rate of 10°C/min from 60 to 800°C.

Porosity of the Porous CS/GO Composite Xerogels

The porosity of the CS/GO composite xerogels was measured with a specific-gravity bottle on the basis of Archimedes' principle. The porosity of the samples was determined as follows:[37]

$$Porosity \ (\%) = [(W_2 - W_3 - W_0)/\rho_e]/[(W_1 - W_3)/\rho_e] \times 100$$

where W_1 is the weight of the specific-gravity bottle filled with ethanol, W_2 is the weight of the specific-gravity bottle including ethanol and the xerogel sample, W_3 is the weight of the specific-gravity bottle when the ethanol saturated xerogel sample has been removed from W_2, W_0 is the weight of the xerogel sample, ρ_e is the density of ethanol, $(W_1 - W_3)/\rho_e$ is the total volume of the xerogel sample including pores, and $(W_2 - W_3 - W_0)/\rho_e$ is the pore volume of the xerogel sample.

In Vitro Swelling and Degradation

For the water absorption analysis, the CS and CS/GO xerogels were first dried to a constant weight (W_0), then immersed in distilled water for 24 h, blotted with filter paper, and weighed again (W_1). The equilibrium water absorption percentage was calculated according to the following equation:[29]

$$Water \ absorption \ (\%) = [(W_1 - W_0)/W_0] \times 100$$

The *in vitro* degradation of the CS and CS/GO xerogels was carried out in PBS (pH = 7.4) at 37°C according to a procedure described elsewhere.[38] Briefly, xerogels of known dry weights (W_d's) were sterilized by immersion in 70% alcohol followed by thorough washing with PBS (pH = 7.4) and incubated in the PBS solution with gentle mechanical agitation (30 rpm) for the period of study. At specified intervals (10, 20, and 30 days), samples were removed from the medium, rinsed with distilled water, filtered, lyophilized, and reweighed (W_t). The degradation was quantified as the change in the sample weight over time. The percentage mass loss is given by

$$Mass \ loss \ (\%) = [(W_d - W_t)/W_d] \times 100\%$$

Mechanical Testing

The compressive strengths of the CS and CS/GO xerogel samples were measured with a universal testing machine (AGS-X5kN, Shimadzu Corp., Japan) at 25°C and 60% relative humidity. The compressive sample was 20 mm in diameter and 50 mm in length. The CS and CS/GO samples were rehydrated in PBS (pH = 7.4) overnight before testing. For the mechanical properties test, the compressive strength was not obtained until the samples were compressed to 50% of their initial height at a crosshead speed of 1 mm/min. To ensure the accuracy and repeatability of data, at least three measurements were carried out for each sample.

Adsorption Behavior of the Porous CS and CS/GO Xerogels for DOX

Each xerogel sample with the same mass (10 mg) was separately put into a 10-mL glass weighing bottle containing DOX solution (5 mL) to adsorb the DOX at room temperature and kept out of the light (DOX was stable in the dark). The concentrations of DOX were 0.15, 0.2, and 0.4 mg/mL, respectively. Every 24 h, the DOX loading efficiency of each sample was measured with a UV spectrophotometer (UV, Specord50, Analytic Jena, Germany) at 480 nm. This was continued for a total of 72 h. (The effect of the time on the adsorption was studied, and the results show that there was no obvious change in adsorption after 72 h. So, 72 h was used for the experiments because it was long enough for the adsorption to reach equilibrium.) The concentration of DOX in the solution was calculated with a
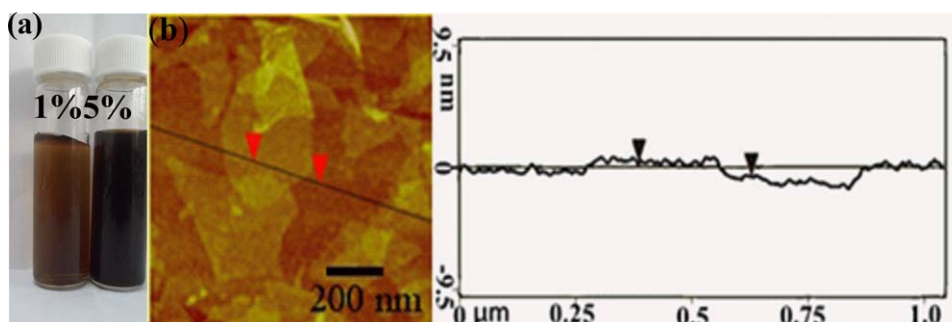
Figure 1. (a) GO aqueous suspensions at concentrations of 1 and 5 wt % and (b) tapping-mode AFM image and height profile of GO. [Color figure can be viewed in the online issue, which is available at wileyonlinelibrary.com.]

standard calibration curve. The adsorption efficiency (A_d) and apparent adsorption capacity (Q_t; mg/g) were obtained according to the following equations:[30]

$$A_d(\%) = (C_0 - C_t)/C_0 \times 100\%$$

$$Q_t = (C_0 - C_t)V/W$$

where C_0 is the initial concentration of DOX (mg/mL), C_t is the concentration of DOX at a given time (mg/mL), W is the weight of the xerogel sample (mg), V represents the volume of the solution (mL), and Q_t is the apparent adsorption capacity of the xerogel at a given time (mg/g), which if given a long enough adsorption period, is equal to the saturation adsorption efficiency (%) and saturation adsorption capacity (mg/g).

Release Test of DOX *In Vitro*
Drug-release experiments were performed to demonstrate the release of the entrapped DOX and to determine the duration and extent of drug release from the composite xerogels. Before the study, each xerogel sample was immersed in a 0.2 mg/mL DOX solution for 3 days, lyophilized, and then immersed in 25 mL of PBS buffer (pH 4.0 and 7.4) in a flask. The flask was sealed, incubated, and stirred at a constant rate at 37°C for a period of 28 days. At selected time intervals, 5 mL of solution was taken out from the flask for testing, and an equal volume of fresh PBS buffer was used to replenish it. The released DOX was evaluated by the measurement of the ultraviolet–visible (UV–vis) absorbance of the extractive solution at $\lambda = 480$ nm. The cumulative release percentage of DOX from the xerogels was calculated with the following equation:[39]

$$\text{Cumulative release} \ (\%) = M_t/M_0 \times 100\%$$

where M_t is the amount of drug released at time t and M_0 is the initial loaded drug amount.

Statistical Analysis
At least three samples were used for the experiments, and the obtained values were expressed as the mean value of at least three replicates and the standard deviation. Statistical analysis was carried out with a one-way analysis of variance, and a value of $p < 0.05$ was considered significant. The error bars denote the standard deviation ($n = 3$).

RESULTS AND DISCUSSION

Characterization of GO
As shown in Figure 1(a), the exfoliated GO was readily dispersed in water to form a stable transparent suspension. The

atomic force microscopy (AFM) image and its corresponding height profile [Figure 1(b)] showed that the measured thickness of the GO sheets was about 0.6–1.2 nm. This suggested that GO was fully exfoliated into individual sheets in water by ultrasonic treatment.

As the transmission electron microscopy picture shows [Figure S1(a)], the as-prepared GO sheets were nearly transparent under electron irradiation; this indicated the GO sheets were quite thin. As shown in Figure S1(b), the C1s X-ray photoelectron spectrum of GO indicated the presence of four components: the C in C=C bonds (284.5 eV), the C in C—O bonds (286.6 eV), the C in C=O bonds (287.7 eV), and the C in O—C=O bonds (288.7 eV). This indicated the considerable degree of oxidation existing in the GO sheets. The existence of the oxygen-functionalized groups resulted in the hydrophilic nature of GO.

Microstructure of the Xerogels
GO consists of graphitic regions interspersed with sp3-hybridized carbons containing —COOH, —OH, and epoxide functional groups. Each unit of CS contains an amino group (—NH$_2$) and two —OH groups. So, the —COOH and —OH groups on the GO sheets could form hydrogen-bonding interactions with —OH and —NH$_2$ groups in CS. As a result, GO was wrapped in CS when they were mixed in an aqueous solution with the aid of sonication.

The lyophilized and neutralized CS xerogel was light white in color, whereas the CS/GO xerogels were black–brown. As the SEM images show, the white pure CS xerogel displayed relatively large pores [Figure 2(a)]. On the contrary, for the CS/GO composite xerogels, the pores turned out to be smaller and more compact after the addition of GO [Figure 2(b–d)]. These indicated that the addition of GO resulted in an increase in the internal pore numbers and the specific surface area of the CS/GO composite xerogels. This increase in the surface area favored DOX adsorption. The relationship between the porosity and the GO content is demonstrated in Figure 3. Comparing the porosity of the CS and CS/GO composite xerogels, no significant statistically difference among the samples was observed ($p > 0.05$). This result indicated that the porosity was not dependent on the GO concentration, and the values were all in the range 84.1–91.5%.

The FTIR spectra of the GO sheets and CS and CS/GO xerogels are given in Figure 4. As shown in Figure 4(a), the spectrum of
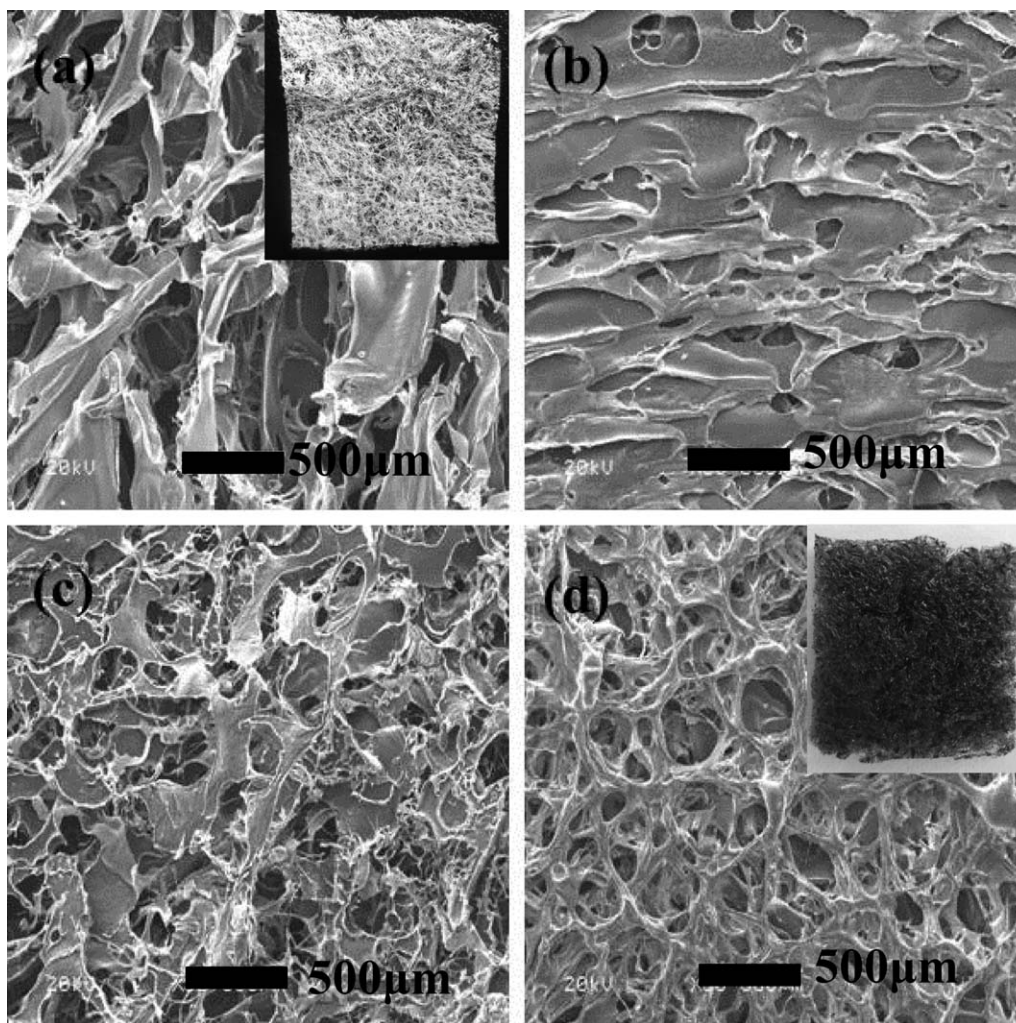
Figure 2. SEM images of the (a) CS, (b) CS/GO (1 wt %), (c) CS/GO (3 wt %), and (d) CS/GO (5 wt %) xerogels. The bars represent 500 μm. The insets are digital images.

GO illustrated the presence of oxygen-containing functional groups. The peaks at 1060, 1246, 1380, and 1600 cm^{-1} corresponded to C—O bonds, C—O—C stretching vibrations, C—OH stretching, and C—C skeletal vibrations of functional graphitic domains,[17,36] whereas the peaks located at 1720 and 3455 cm^{-1} corresponded to C—O stretching vibrations of the —COOH groups and O—H stretching vibrations, respectively. These functional groups made GO highly hydrophilic and dispersible. For the CS xerogel [Figure 4(b)], the curve showed symmetric stretching vibrations of the N—H bond at 3440 cm^{-1}, stretching vibrations of C—H bond at 2923 and 2853 cm^{-1}, stretching vibrations of C=O bond (amide I) at 1636 cm^{-1}, bending vibrations of C—H bond at 1420 cm^{-1}, and asymmetric stretching vibrations and symmetric stretching vibrations of C—O—C bond at 1153, 1088, and 1031 cm^{-1}. Compared with the spectrum of the pure CS sample, the CS/GO composite xerogel showed an obvious increased absorption band at 1600 cm^{-1}, which indicated that the GO phase was successfully added to the CS matrix.
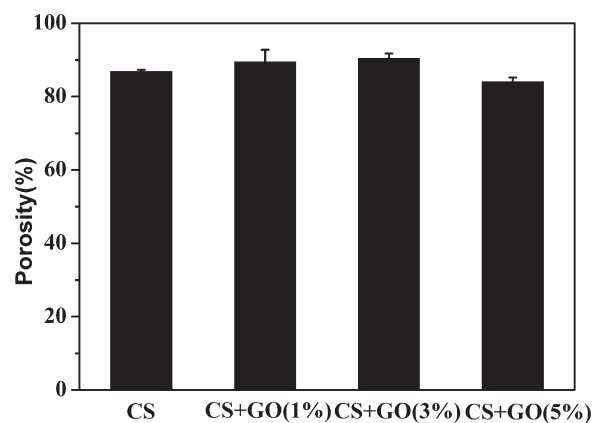

Figure 3. Porosity of the CS, CS/GO (1 wt %), CS/GO (3 wt %), and CS/GO (5 wt %) xerogels. In a comparison of the porosities of the CS and CS/GO composite xerogels, no statistically significant difference was observed among the samples. The values are the means and standard deviations ($p > 0.05$, $n = 3$).
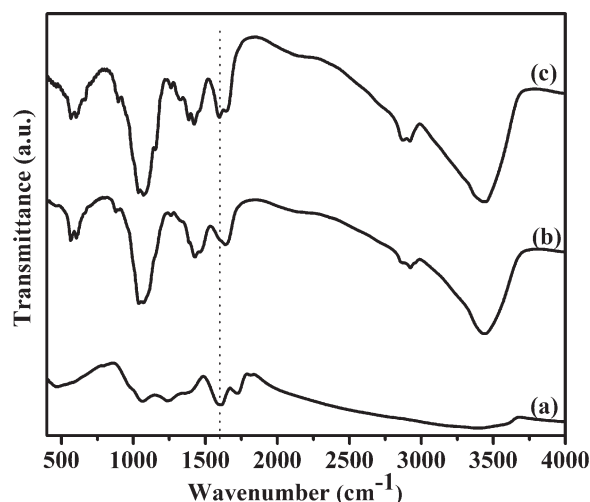
Figure 4. FTIR spectra of (a) GO, (b) the CS xerogel, and (c) the CS/GO (5 wt %) composite xerogel.

Figure 6. TGA curves of the CS, CS/GO (1 wt %), CS/GO (3 wt %), and CS/GO (5 wt %) xerogels. [Color figure can be viewed in the online issue, which is available at wileyonlinelibrary.com.]

The XRD patterns of the GO sheets and the CS and CS/GO (5 wt %) xerogels are shown in Figure 5. The GO sample displayed a strong (002) diffraction peak at 10.9°, which corresponded to a c-axis spacing of 0.81 nm. On the contrary, both the CS and CS/GO xerogels [Figure 5(b,c)] exhibited a broad peak centered 20.3°, which indicated the generally amorphous state of the CS-based xerogels. The two XRD patterns were exactly the same; this demonstrated the formation of a fully exfoliated structure of GO sheets in the CS matrix and the disappearance of the regular and periodic structure of GO.[40] In addition, this identity also implied that the addition of a small quantity of GO did not affect the crystallinity of CS.

TGA of the CS/GO Xerogels

TGA is a standard technique for determining thermal stability of the composition materials. Figure 6 shows the TGA curves of the CS and CS/GO xerogels obtained under a nitrogen atmosphere; this suggested that GO had almost no significant effect on the thermal stability of the CS material at low concentra-
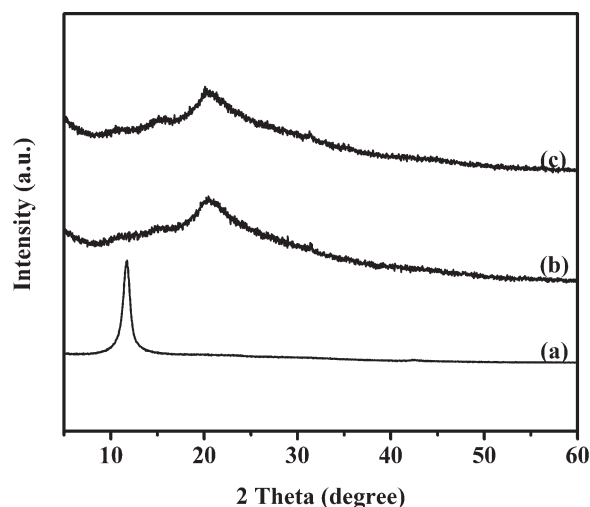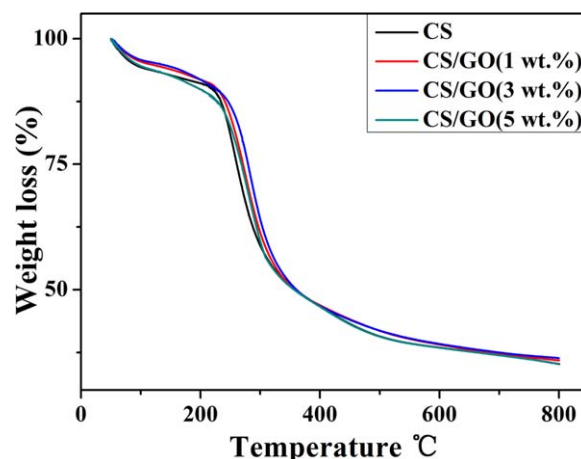
tions. There was a mass loss of about 5% before 100°C that was due to the evaporation of the water. Then, the first rapid weight loss was observed from 100 to 225°C and was due to the dehydration of the CS and CS/GO xerogels and the decomposition of the relatively low-molecular-weight CS. The second weight loss between 225 and 450°C represented the decomposition of the polymeric material. As the temperature increased further, the xerogels showed almost no larger change in weight.

In Vitro Swelling and Biodegradation Study

The equilibrium swelling, water absorption, and shape retention are critical for implant materials. The water absorption of porous xerogels is shown in Figure 7 and indicates that the incorporation of GO had a significant effect on the water absorption ability. As the proportion of the GO grew to 5 wt %, the water absorption gradually increased from 2400 to 3600%. This may have been because the pore sizes became smaller with the addition of GO, as shown in the SEM images, and the specific surface area increased. So the amount of the water absorbed through capillary action also increased.
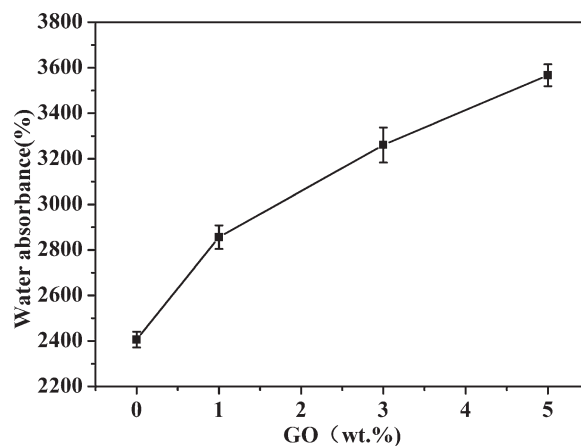

Figure 5. XRD patterns of (a) GO, (b) the CS xerogel, and (c) the CS/GO (5 wt %) composite xerogel.

Figure 7. Water absorbances of the CS, CS/GO (1 wt %), CS/GO (3 wt %), and CS/GO (5 wt %) xerogels. The values are the means and standard deviations ($n = 3$).

Figure 8. Shape changes in the CS, CS/GO (1 wt %), CS/GO (3 wt %), and CS/GO (5 wt %) xerogels. [Color figure can be viewed in the online issue, which is available at wileyonlinelibrary.com.]

Moreover, —OH and —COOH groups on the GO sheets strengthened the hydrophilicity and water permeability of the porous materials, and these functional groups were involved in the hydrogen-bonding interactions with the —NH$_2$ and —OH groups of the CS molecules. With the further addition of GO, more extensive crosslinks were created, and these interactions acted as a kind of physical crosslink and increased the water absorbance. Obviously, high water absorption abilities should have facilitated the absorbability of DOX molecules to the surface and interior regions of the porous CS/GO xerogels, which should have then led to high drug-loading abilities.

Figure 8 summarizes the shape retention in terms of the xerogel shape as a function of the immersion time in PBS (pH 7.4) with a weak external force. The pure CS and CS/GO xerogels experienced swelling, and the CS/GO xerogels retained their overall sizes and shapes in the first 15 days, but pure CS gradually disintegrated and almost collapsed in the first 15 days. This result suggests that the porous CS/GO xerogels had a good wet strength and wet-state stability, which would be beneficial to their applications *in vivo*.

A porous implantable delivery system is expected to naturally disintegrate as the in-growth of tissue takes place. Thus, the degradation time of the implantable materials affects the implantation site and the slow controlled release effect of the drug. As shown in Figure 9, the contents of CS, CS/GO (1 wt %), CS/GO (3 wt %), and CS/GO (5 wt %) remaining after 30 days of immersion in PBS (pH 7.4) were 70, 72.5, 79.8, and 80.1%, respectively. This illustrated that the addition of GO lowered the degradation rate of CS because of the strong interactions between CS and GO. It should be mentioned that at 30 day, the differences in the weight loss profile of the four sets of materials did not consider the effect of enzymes. It is well known that in human serum, the mass loss behavior of CS matrices includes simple dissolution and enzyme degradation. As reported by Freier et al.,[38] CS is mainly depolymerized enzy-

matically by lysozyme and not by other enzymes. However, at 35 days, the CS and CS/GO samples had completely collapsed in the PBS solution, as shown in Figure S2. Thus, we propose that with enzyme addition, the degradation rate was enhanced significantly, and the structure was seriously destroyed.

Mechanical Testing

Figure 10 shows the compressive strength of the CS/GO xerogels in the dry and wet states with different GO contents when the samples were compressed by 50%. The CS/GO xerogels exhibited a gradual increase in the compressive strength with increasing GO content. This increase was attributed to the good compatibility between CS and GO and H-bonding interactions between the oxygen-containing groups (e.g., —OH, —COOH and epoxides) of the GO nanosheets and the —OH/—NH$_2$ groups of CS.[41] These factors gave rise to nanosheet–polymer interactions that provided better load transfers between the CS matrix and the GO sheets; this was beneficial for mechanical improvements. Comparing the compressive strength of the CS/GO (5 wt %) xerogels with those of other samples, we observed a significant statistically difference among the samples ($p < 0.05$); and GO (5 wt %) resulted in a larger compressive strength of the CS/GO xerogels in the dry and wet states. As shown in Figure 10(b), the compressive strength of the CS/GO (5 wt %) xerogel was nearly three times higher than that of the CS xerogel. From an application point of view, the strength in the wet state is more important for drug adsorbents and *in vivo* drug release.

Adsorption Ability of the CS/GO Xerogels for DOX

Figure 11 shows the saturated adsorption capacity and efficiency of the CS/GO xerogels with different GO contents at different original DOX concentrations, which were calculated according to the difference in the DOX concentrations between the original DOX solution and the eventual solution after 72 h with UV–vis spectra at 480 nm. The results indicate that the adsorption capacity increased with increasing initial DOX concentration. For example, the adsorption capacity of the CS/GO (5 wt %) composite xerogel for DOX was up to 69 mg/g at a DOX concentration of 0.15 mg/mL, 98 mg/g at a DOX concentration of 0. 2 mg/mL, and 126.3 mg/g at a DOX concentration of 0.4
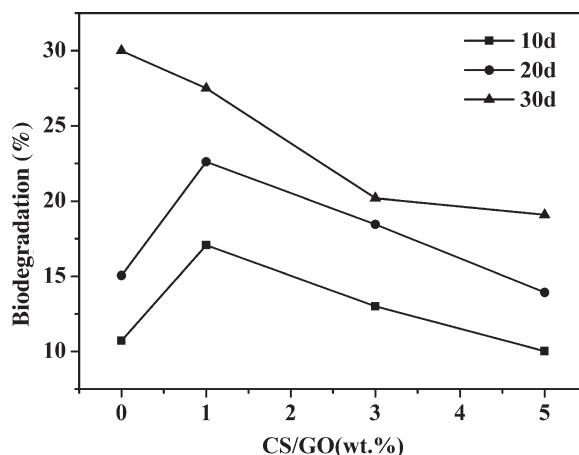

Figure 9. Mass losses of the CS, CS/GO (1 wt %), CS/GO (3 wt %), and CS/GO (5 wt %) xerogels.
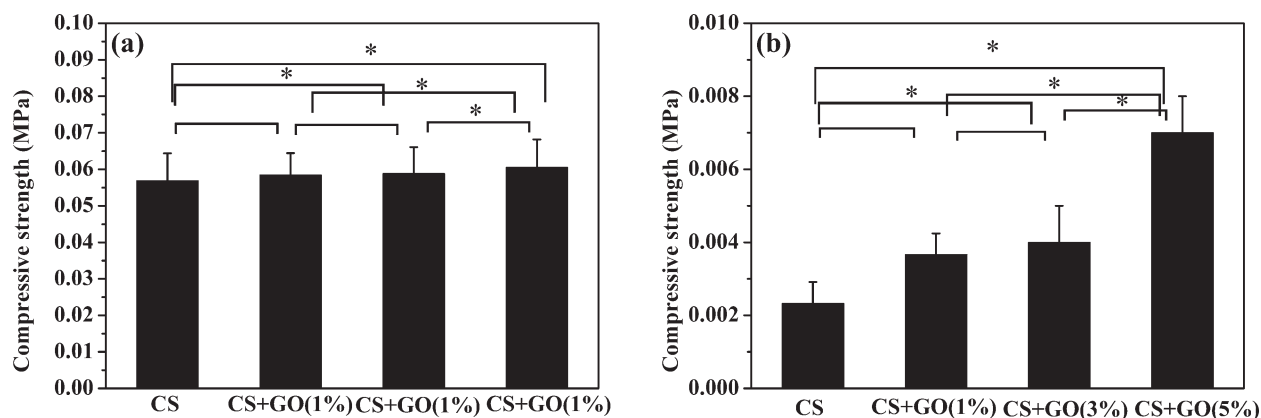
Figure 10. Compressive strengths of the CS, CS/GO (1 wt %), CS/GO (3 wt %), and CS/GO (5 wt %) xerogels in the (a) dry and (b) wet states. The values are the means and standard deviations (*$p < 0.05$, $n = 3$).

mg/mL [Figure 11(a)], although A_d did not follow this trend and was 92.1% at a DOX concentration of 0.15 mg/mL, 98.1% at a DOX concentration of 0.2 mg/mL, and 63.1% at a DOX concentration of 0.4 mg/mL [Figure 11(b)]. The results indicate that A_d in the CS/GO (5 wt %) composite xerogel in the 0.2 mg/mL DOX solution was the highest. Thus, we chose this DOX concentration to examine the effect of the GO content on the adsorption ability of the CS/GO xerogels.

Like CS, DOX contains abundant —NH$_2$, —OH, and phenolic groups. Thus, hydrogen bonding between the two components was formed when the CS and CS/GO xerogels were immersed in DOX solutions. In addition, the large π-conjugated structure of the exposed GO sheets could form π–π stacking interactions with the quinone portion of DOX and the hydrophobic effect between them. As Figure 11 shows, the saturated adsorption capacity and efficiency of the CS/GO xerogels for DOX gradually increased with increasing GO content. When 5 wt % GO was incorporated, the saturated adsorption capacity increased about 240% compared with that of the pure CS xerogel. This could be explained by the fact that the addition of GO increased the surface area of the porous CS xerogel and caused more functional groups (e.g., —OH and —NH$_2$ groups) to be exposed to outside; this enhanced the

adsorption ability of the CS/GO xerogels. Convincing evidence came from the UV–vis spectroscopy on DOX aqueous solutions adsorbed by the CS/GO (5 wt %) xerogel at different times, as shown in Figure S3. As the spectra show, the specific absorption peak of DOX at $\lambda = 480$ nm became gradually weaker with time; this confirmed the DOX adsorption behavior of the CS/GO xerogel.

The effect of the GO content on the adsorption capacity of the CS/GO xerogels for DOX was also verified by the change in color of the DOX solutions immersed with the CS/GO xerogels, as shown in Figure 12. As time went by, DOX was gradually adsorbed by the xerogels, and the color in all of the solutions turned lighter. The first 24 h showed the fastest adsorption speed. For example, the CS/GO (5 wt %) xerogel exhibited about 72.5% A_d, which was measured by UV–vis spectroscopy and calculated according to a standard curve of DOX absorbance to its concentration (Figure S4). After this stage, the color of the solutions immersed with the CS/GO (3 wt %) and CS/GO (5 wt %) xerogels showed an obvious change. Seventy-two hours later, the color of the solutions from left to right was from deep to shallow. The solution immersed in the CS/GO (5 wt %) xerogel was almost colorless, and about 98.1% DOX in the solution was absorbed by the xerogel. This indicated that
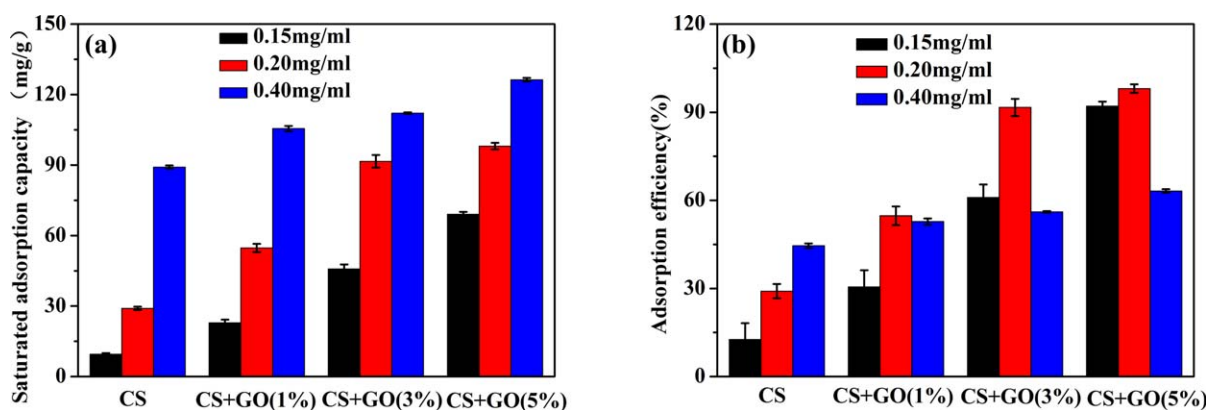

Figure 11. (a) Saturated adsorption capacities and (b) A_d values of the CS, CS/GO (1 wt %), CS/GO (3 wt %), and CS/GO (5 wt %) xerogels at different original DOX concentrations. The values are the means and standard deviations ($n = 3$). [Color figure can be viewed in the online issue, which is available at wileyonlinelibrary.com.]
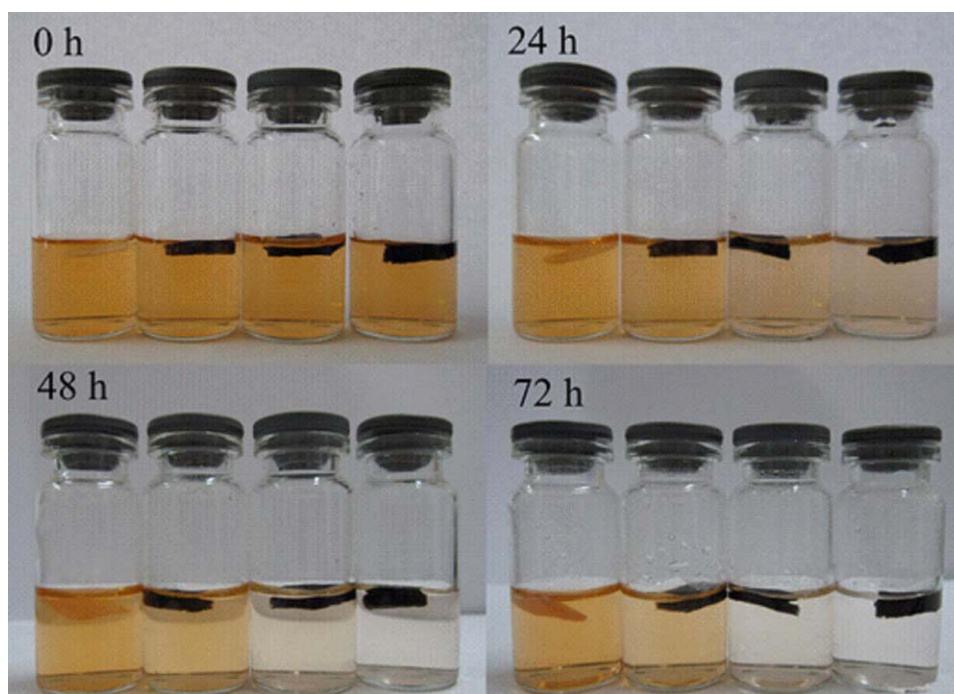
Figure 12. Digital photographs of the adsorption process of the CS and CS/GO xerogels for DOX at 0.2 mg/mL at different times: the pure CS xerogel and the CS/GO (1 wt %), CS/GO (3 wt %), and CS/GO (5 wt %) xerogels (from left to right). [Color figure can be viewed in the online issue, which is available at wileyonlinelibrary.com.]

the DOX adsorption ability of the CS/GO composite xerogels was directly proportional to the GO content.

In Vitro Drug Release

Figure 13 shows the cumulative DOX release from the pure CS xerogel and CS/GO composite xerogels with different GO contents as a function of the immersion time up to 28 days. As the plots show in Figure 13, the first 7 days showed the fastest release rate. The release percentages of DOX at pH 7.4 were about 26.1, 21.7, 19.3, and 17.75% for the pure CS, CS/GO (1 wt %), CS/GO (3 wt %), and CS/GO (5 wt %) xerogels, respectively. Similarly the release percentages at pH 4 were about 39.0,

36.8, 31.4, and 29.3% for the pure CS, CS/GO (1 wt %), CS/GO (3 wt %), and CS/GO (5 wt %), respectively. After that, the release rate slowed down for each sample, and the release rate gradually declined under neutral (pH = 7.4) and acidic (pH = 4) buffers with the increase of GO content. These results indicate that the CS/GO composite xerogels with higher GO contents possessed better DOX slow-release abilities. This was ascribed to the hydrogen-bonding interaction and π–π stacking interaction between DOX and GO, which could have resulted in the controlled release. However, the release behaviors under neutral and acidic conditions indicated that the total release amount of DOX expressed pH-dependent behavior and was
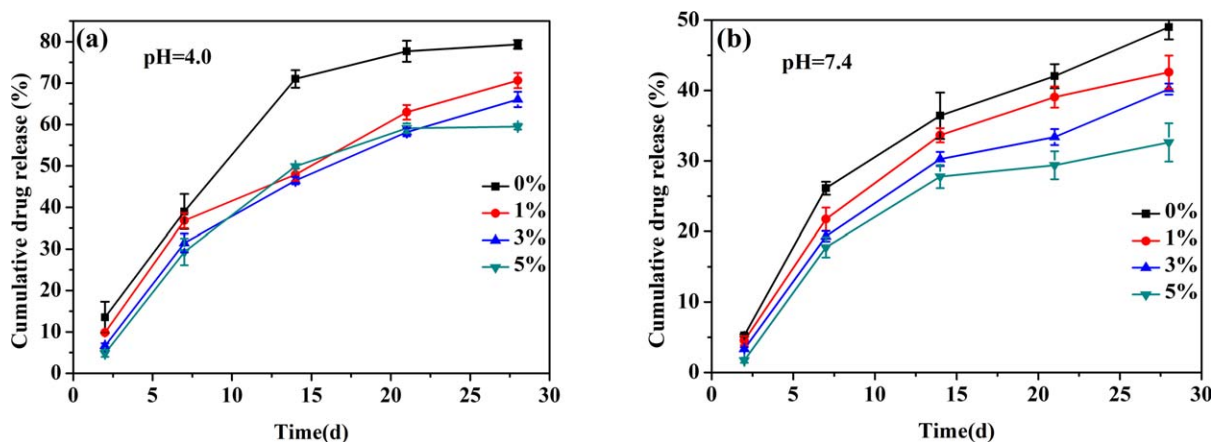

Figure 13. In vitro release of DOX from the CS and CS/GO composite xerogels with different GO contents in (a) pH 4 and (b) pH 7.4 PBS at 37°C with immersion times up to 28 days. The values are the means and standard deviations ($n = 3$). [Color figure can be viewed in the online issue, which is available at wileyonlinelibrary.com.]

much higher under acidic conditions than under neutral conditions. This characteristic may have come about because the —NH$_2$ groups of DOX were protonated under acidic conditions; this resulted in the partial dissociation of hydrogen-bonding interactions. Hence, the amount of released DOX was much higher.[26,42] Many pathological processes in tumor tissue and intracellular endosome/lysosome are accompanied with a local pH decrease by 1–2.5 pH units in comparison with that (pH 7.4) in blood and normal tissues.[43,44] Herein, the CS/GO xerogels, as pH-responsive composite materials, not only responded to the changes in the environmental pH but also allowed on-site modulation of the pH response for enhanced drug delivery.

CONCLUSIONS

Highly porous CS/GO composite xerogels were prepared by a simple and green freeze-drying method. The as-made xerogels exhibited efficient adsorption and slow-release abilities of the DOX molecules. Moreover, the GO content showed obvious influences on the adsorption and release abilities. In other words, an increase in the GO content resulted in increases in the adsorption and slow-release abilities. In addition, the drug release was pH sensitive, and the CS/GO xerogels exhibited higher drug releases under acidic conditions than under neutral conditions. This was mainly due to the reduced hydrogen-bonding interaction between DOX and the drug carrier under acidic conditions. On the basis of the biodegradable characteristic of CS, the low cost of GO, and the facile preparation and efficient drug-delivery ability of the CS/GO composite xerogels, such CS/GO xerogels loaded with the drug DOX seem to be a promising carrier material for use as implantable drug-delivery systems for long-term bone-disease control.

ACKNOWLEDGMENTS

REFERENCES

1. Itokazu, M.; Kumazawa, S.; Wada, E.; Wenyi, Y. *Cancer Lett.* **1996**, *107*, 11.

2. Fan, H.; Dash, A. *Int. J. Pharm.* **2001**, *213*, 103.

3. Kursawe, M.; Glaubitt, W.; Thierauf, A. *J. Sol–Gel Sci. Technol.* **1998**, *13*, 267.

4. Kim, J. H.; Kim, Y. S.; Park, K.; Kang, E.; Lee, S.; Nam, H. Y.; Kim, K.; Park, J. H.; Chi, D. Y.; Park, R. W.; Kim, I. S.; Choi, K.; Kwon, I. C. *Biomaterials* **2008**, *29*, 1920.

5. Mao, H. Q.; Roy, K.; Troung-Le, V. L.; Janes, K. A.; Lin, K. Y.; Wang, Y.; August, J. T.; Leong, K. W. *J. Controlled Release* **2001**, *70*, 399.

6. Säkkinen, M.; Linna, A.; Ojala, S.; Jürjenson, H.; Veski, P.; Marvola, M. *Int. J. Pharm.* **2003**, *250*, 227.

7. Kim, I. Y.; Seo, S. J.; Moon, H. S.; Yoo, M. K.; Park, I. Y.; Kim, B. C.; Cho, C. S. *Biotechnol. Adv.* **2008**, *26*, 1.

8. Varma, A. J.; Deshpande, S. V.; Kennedy, J. F. *Carbohydr. Polym.* **2004**, *55*, 77.

9. Volda, I. M. N.; Varum, K. M.; Guibal, E.; Smidsrod, O. *Carbohydr. Polym.* **2003**, *54*, 471.

10. Allen, M. J.; Tung, V. C.; Kaner, R. B. *Chem. Rev.* **2010**, *110*, 132.

11. Geim, A. K. *Science* **2009**, *324*, 1530.

12. Rao, C. N. R.; Sood, A. K.; Subrahmanyam, K. S.; Govindaraj, A. *Angew. Chem. Int. Ed.* **2009**, *48*, 7752.

13. Park, S.; Ruoff, R. S. *Nat. Nanotechnol.* **2009**, *4*, 217.

14. Chen, H.; Muller, M. B.; Gilmore, K. J.; Wallace, G. G.; Li, D. *Adv. Mater.* **2008**, *20*, 3557.

15. Stankovich, S.; Dikin, D. A.; Piner, R. D.; Kohlhaas, K. A.; Kleinhammes, A.; Jia, Y.; Wu, Y.; Nguyen, S. B. T.; Ruoff, R. S. *Carbon* **2007**, *45*, 1558.

16. Schniepp, H. C.; Li, J. L.; McAllister, M. J.; Sai, H.; Herrera-Alonso, M.; Adamson, D. H.; Prud'homme, R. K.; Car, R.; Saville, D. A.; Aksay, I. A. *J. Phys. Chem. B* **2006**, *110*, 8535.

17. Si, Y. C.; Samulski, E. T. *Nano Lett.* **2008**, *8*, 1679.

18. Li, D.; Muller, M. B.; Gilje, S.; Kaner, R. B.; Wallace, G. G. *Nat. Nanotechnol.* **2008**, *3*, 101.

19. Chang, Y. L.; Yang, S. T.; Liu, J. H.; Dong, E.; Wang, Y. W.; Cao, A.; Liu, Y. F.; Wang, H. F. *Toxicol. Lett.* **2011**, *200*, 201.

20. Zhang, X. Y.; Hu, W. B.; Li, J.; Tao, L.; Wei, Y. *Toxicol. Res.* **2012**, *1*, 62.

21. Liao, K. H.; Lin, Y. S.; Macosko, C. W.; Haynes, C. L. *ACS Appl. Mater. Interfaces* **2011**, *3*, 2607.

22. Liu, Z.; Robinson, J. T.; Sun, X. M.; Dai, H. J. *J. Am. Chem. Soc.* **2008**, *130*, 10876.

23. Hu, W. B.; Chen, P.; Lv, M.; Li, X. M.; Zhang, Y. J.; Chen, N.; Fan, C. H.; Hua, Q. *ACS Nano* **2011**, *5*, 3693.

24. Magrez, A.; Kasas, S.; Salicio, V.; Pasquier, N.; Seo, J. W.; Celio, M.; Catsicas, S.; Schwaller, B.; Forro, L. *Nano Lett.* **2006**, *6*, 1121.

25. Yang, K.; Li, Y. J.; Tan, X. F.; Peng, R.; Liu, Z. *Small* **2012**, *9*, 1492.

26. Bao, H.; Pan, Y.; Ping, Y.; Sahoo, N. G.; Wu, T.; Li, L.; Li, J.; Gan, L. H. *Small* **2011**, *7*, 1569.

27. Rana, V. K.; Choi, M. C.; Kong, J. Y.; Kim, G. Y.; Kim, M. J.; Kim, S. H.; Mishra, S.; Singh, R. P.; Ha, C. S. *Macromol. Mater. Eng.* **2011**, *296*, 131.

28. Pan, Y.; Wu, T.; Bao, H.; Li, L. *Carbohydr. Polym.* **2011**, *83*, 19085.

29. Depan, D.; Girase, B.; Shah, J. S.; Misra, R. D. K. *Acta Biomater.* **2011**, *7*, 3432.

30. Zhang, N.; Qiu, H.; Si, Y.; Wang, W.; Gao, J. *Carbon* **2011**, *49*, 827.

31. He, Y. Q.; Zhang, N. N.; Wang, X. D. *Chin. Chem. Lett.* **2011**, *22*, 859.

32. Gabizon, A.; Shmeeda, H.; Barenholz, Y. *Clin. Pharm.* **2003**, *42*, 419.

33. Nakanishi, T.; Fukushima, S.; Okamoto, K.; Suzuki, M.; Matsumura, Y.; Yokoyama, M.; Okano, T.; Sakurai, Y.; Kataoka, K. *J. Controlled Release* **2001**, *74*, 295.

34. Yoo, H. S.; Lee, K. H.; Oh, J. E.; Park, T. G. *J. Controlled Release* **2000**, *68*, 419.

35. Nori, A.; Jensen, K. D.; Tijerina, M.; Kopeckova, P.; Kopecek, J. *Bioconjugate Chem.* **2003**, *14*, 44.

36. Xu, Y.; Bai, H.; Lu, G.; Li, C.; Shi, G. *J. Am. Chem. Soc.* **2008**, *130*, 5856.

37. Pati, F.; Adhikari, B.; Dhara, S. *J. Mater. Sci.: Mater. Med.* **2012**, *23*, 1085.

38. Freier, T.; Koh, H. S.; Kazazian, K.; Shoichet, M. S. *Biomaterials* **2005**, *26*, 5872.

39. Ekici, S.; Saraydin, D. *Polym. Int.* **2007**, *56*, 1371.

40. Du, X. S.; Xiao, M.; Meng, Y. Z.; Hay, A. S. *Carbon* **2005**, *43*, 195.

41. Yang, X.; Zhang, X.; Liu, Z.; Ma, Y.; Huang, Y.; Chen, Y. *J. Phys. Chem. C* **2008**, *112*, 17554.

42. Depan, D.; Shah, J.; Misra, R. D. K. *Mater. Sci. Eng. C* **2011**, *31*, 1305.

43. Tannock, I. F.; Rotin, D. *Cancer Res.* **1989**, *49*, 4373.

44. Zhou, T.; Xiao, C. F.; Chen, S. M.; Shen, J.; Wu, W. T.; Zhou, S. H. *Acta Biomater.* **2013**, *9*, 4546.